

Van der Waals Complexes between Boron Trifluoride and Carbon Monoxide in Liquefied Argon: An Infrared Study

E. J. Sluys and B. J. van der Veken*

Contribution from the Department of Chemistry, Universitair Centrum Antwerpen, Groenenborgerlaan 171, B2020 Antwerp, Belgium

Received February 9, 1995[⊗]

Abstract: Infrared spectra have been recorded of solutions in liquefied argon (85–115 K) containing both boron trifluoride and carbon monoxide. The formation of complex species was concluded from the appearance of bands not attributable to the monomer molecules. Using concentration variation, bands due to the 1:1 complex $\text{BF}_3 \cdot \text{CO}$ and to the 1:2 complex $\text{BF}_3 \cdot (\text{CO})_2$ have been identified. From temperature-dependant studies, the enthalpy of formation of the 1:1 complex was found to be -7.6 ± 0.3 and -14.5 ± 1.0 kJ mol⁻¹ for the 1:2 complex. A very weak band, presumably due to a third complex, is tentatively assigned to the 1:1 complex $\text{BF}_3 \cdot \text{OC}$ in which CO is binding to the boron atom via its oxygen atom. The solvent shifts of ν_2 and ν_3 of BF_3 and the complexation shifts of these modes are interpreted in terms of a simple induction model.

Introduction

From the boron trihalides, the trifluoride is the weakest Lewis acid,¹ due to the π -back-bonding from fluorine to the boron atom.² Also, the Lewis base carbon monoxide is a poor σ donor.³ As a consequence, in room temperature gas mixtures of BF_3 and CO, the adduct $\text{BF}_3 \cdot \text{CO}$ does not form in measurable quantities,⁴ and its concentration can be increased, making the species amenable to investigation, in a cryogenic environment only.

The adduct was first investigated using molecular beam electric resonance spectroscopy.⁵ The authors found that the CO molecule binds to the boron atom via the carbon lone pair, with the B–C bond quite long, 2.886(5) Å, reflecting the weakness of the interaction. The BF_3 moiety was found to deviate only slightly from planarity, the C–B–F angle being 90.65(25)°. In a matrix isolation infrared study,⁶ the symmetric BF_3 stretch of the complex, which is symmetry forbidden in the BF_3 monomer, was not observed: this is in line with the small distortion from planarity of the BF_3 moiety. More recently, high-resolution infrared spectra of the adduct formed in a jet expansion have been discussed,⁷ and renewed matrix isolation measurements, combined with *ab initio* calculations at the 6-31G level, have been performed.⁸ *Ab initio* calculations at the MP2/TZ2P level have been discussed.⁹ These authors found agreement of their calculated B–C bond length with the experimental value, and it was stressed that the dissociation

energy of the complex is low, and that the bonding in this complex is virtually solely due to electrostatic interactions.

From the above it is clear that the structure of $\text{BF}_3 \cdot \text{CO}$ is firmly established, but that other characteristics of the species are less well documented, mainly because the adduct was investigated under nonequilibrium conditions.

The near-planarity of the 1:1 complex leaves one side of the boron atom unprotected in very much the same geometrical circumstances as in the BF_3 monomer. As the interaction is electrostatic,⁹ the carbon free electron pair will not nearly saturate the electron deficiency of the boron atom. Therefore, it must be expected that $\text{BF}_3 \cdot \text{CO}$ is capable of binding a second CO molecule, leading to a trigonal bipyramidal 1:2 complex, and that the binding energy of the second CO molecule will be similar to that of the first. Finally, the Lewis structure of CO also suggests that the oxygen atom should be capable of acting as the electron donor, and it cannot be excluded *a priori* that an adduct of the type $\text{BF}_3 \cdot \text{OC}$ is formed, in which CO binds via the oxygen atom. Neither the 1:2 complex nor the OC complex has been observed before.

In cryogenic solutions, Van der Waals complexes are formed under equilibrium conditions,¹⁰ so that thermodynamic data can be obtained. Therefore, in this study, the interaction between BF_3 and CO has been studied in liquefied argon, using infrared spectroscopy.

Experimental Section

Boron trifluoride was obtained from Union Carbide (CP grade), and carbon monoxide (99.997 vol %) was purchased from Messer Griesheim. The solvent gas, argon, was supplied by L'Air Liquide and has a stated purity of 99.9999%. In the vapor phase spectra of the CO and Ar used, no impurities could be detected, while SiF_4 was present as an impurity in the BF_3 used. All gases were used without further purification.

The spectra were recorded at 0.5-cm⁻¹ resolution on a Bruker IFS 66v Fourier transform spectrometer. The liquid noble gas cell and the procedure for preparing the solutions have been described before.¹¹

Accurate frequencies of the band maxima for ν_3 and ν_2 were determined as the minima in the second-derivative spectrum. The

[⊗] Abstract published in *Advance ACS Abstracts*, December 15, 1995.

(1) Greenwood, N. N.; Earnshaw, A. *Chemistry of the Elements*; Pergamon Press: Oxford, 1984; p 223.

(2) Cotton, F. A.; Wilkinson, G. *Advanced Inorganic Chemistry*, 5th ed.; J. Wiley and Sons: New York, 1988; p 175.

(3) Owen, S. M.; Brooker, A. T. *A Guide to Modern Inorganic Chemistry*; Longman Scientific and Technical: Harlow, UK, 1991; p 232.

(4) Shriver, D. F.; Atkins, P. W.; Langford, C. H. *Inorganic Chemistry*, 2nd ed.; Oxford University Press: Oxford, 1994; p 486.

(5) Janda, K. C.; Bernstein, L. S.; Steed, J. M.; Novick, S. E.; Klemperer, W. *J. Am. Chem. Soc.* **1978**, *100*, 8074–8079.

(6) Gebicki, J.; Liang, J. *J. Mol. Struct.* **1984**, *117*, 283–286.

(7) Lee, G.-H.; Takami, M. *J. Chem. Phys.* **1993**, *98*, 3612–3619. Lee, G.-H.; Takami, M. *J. Mol. Struct.* **1995**, *352/353*, 417–422.

(8) Nxumalo, L. M.; Ford, T. A. In *Proceedings of the 9th International Conference on Fourier Transform Spectroscopy*; Bertie, J. E., Wieser, H., Eds.; SPIE: Washington, 1993; pp 200–201.

(9) Jonas, V.; Frenking, G.; Reetz, M. T. *J. Am. Chem. Soc.* **1994**, *116*, 8741–8753.

(10) Van der Veken, B. J.; De Munck, F. R. *J. Chem. Phys.* **1992**, *97*, 3060–3071.

(11) Sluys, E. J.; Herrebout, W. A.; Van der Veken, B. J. *J. Mol. Struct.* **1994**, *317*, 49–57.

Table 1. Infrared Absorption Bands, in cm⁻¹, of ¹⁰BF₃ and ¹¹BF₃ in Liquid Argon at 108 K

assignment	¹⁰ BF ₃	¹¹ BF ₃
2ν ₃ + ν ₁	3866 vv	3763 vv
2ν ₁ + ν ₃	3253 vv	3203 vv
2ν ₃	2989 w	2887 w
ν ₁ + ν ₃ + ν ₄	2850 vv	2799 vv
2ν ₁ + 2ν ₄		2706 ^b vv
ν ₁ + ν ₃	2375 m	2325 ms
2ν ₁ + ν ₄		2236 ^b vw
ν ₃ + ν ₄	1974 vv	1922 vw
ν ₁ + 2ν ₄		1833 ^b vv
ν ₁ + ν ₂	<i>c</i>	1561 vv
ν ₃	1496 vvs	1445 vvs ^d
ν ₁ + ν ₄		1358 ^b s
ν ₂	708 s	681 vs ^e
ν ₄		474 ^b ms ^f

^a w = weak; m = medium; s = strong; v = very. ^b Isotopic splitting not observed. ^c Not observed. ^d BF₃ antisymmetric stretch. ^e Out-of-plane deformation. ^f FBF bend.

Table 2. Temperature Gradients, in cm⁻¹ K⁻¹, for ν₂ and ν₃ Bands in BF₃ and Its CO Complexes in Liquid Argon

	BF ₃	BF ₃ ·CO	BF ₃ ·(CO) ₂
ν ₃ (¹⁰ B)	0.0471	0.0696	
ν ₃ (¹¹ B)	0.0433		
ν ₂ (¹⁰ B)	0.0652		
ν ₂ (¹¹ B)	0.0611	0.1262	0.2075

uncertainties on band maxima are estimated to be near 0.05 cm⁻¹, with those for ν₃ somewhat smaller than those for ν₂.

Results

A. Boron Trifluoride. The vibrational spectra of BF₃ in liquified argon have not been discussed before. Therefore, the frequencies of the bands observed at 108 K, rounded to the nearest wavenumber, together with their assignments, are given in Table 1.

From the amount of BF₃ that could be completely dissolved in liquified argon, the solubility was found to be relatively low, 2 × 10⁻³ M at the lowest temperature investigated, 85 K, but rising sharply with temperature. The low solubility prevented very concentrated solutions from being investigated at this temperature.

When the temperature is increased, all bands undergo a blue shift, which, in the interval studied, is very linear with temperature. The gradients for the ν₂ and ν₃ fundamentals, obtained from a linear regression using accurately determined band maxima, are collected in Table 2.

In solid matrices, the dimer (BF₃)₂ has been observed.⁸ Special attention was devoted to detecting this type of complex in our solutions. However, even in the spectra at the lowest temperatures of the more concentrated solutions no bands attributable to a new species could be observed. Hence, it is concluded that in the solutions used, the concentration of dimers was below the detection limit.

B. BF₃/CO Mixtures. For the solutions containing both BF₃ and CO, the formation of adducts was promoted by using a large excess of CO, which is quite soluble in argon.¹¹

The infrared spectrum in the region of ν₃ of ¹⁰BF₃, recorded at 85 K from a solution containing approximately 5 × 10⁻⁴ M BF₃ and 3 × 10⁻¹ M CO, is compared with the spectrum of a solution containing only BF₃ and that of a solution containing only CO in Figure 1. New bands at 1489 and 1486 cm⁻¹ in the spectrum of the mixed solution prove that at least two complex species are formed. This is confirmed by the appearance of two new bands near other fundamentals of BF₃.

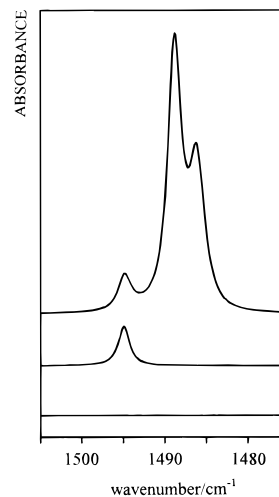


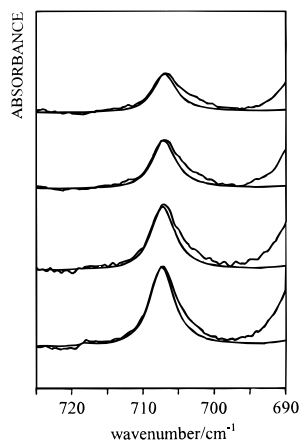
Figure 1. The region of the BF₃ antisymmetric stretch of liquified argon solutions, at 85 K: (top) solution containing BF₃ and CO; (middle) solution containing only BF₃; (bottom) solution containing only CO. The concentrations used are 3 × 10⁻¹ M for CO and 5 × 10⁻⁴ M for BF₃.

The relative intensities in the complex doublets are concentration dependent, i.e., the complexes have different stoichiometries. Assuming thermodynamic equilibrium, and assuming the absorptivities of the bands do not vary over the concentration range studied, the changes in relative intensities were used to derive the stoichiometries of the species.¹⁰ In short, the intensity of a band due to (BF₃)_m(CO)_n is plotted against the product of the *x*-th power of the intensity of a band due to BF₃ and the *y*-th power of the intensity of a CO band, for various integer values of *x* and *y*. The values of *x* and *y* that produce a linear plot correspond to the stoichiometry indices *m* and *n*, respectively. Mixed solutions were investigated, at 90 K, in which the BF₃ concentrations were varied between 1 × 10⁻⁴ and 5 × 10⁻³ M, and those of CO between 6 × 10⁻³ and 3 × 10⁻¹ M. For the concentrated CO solutions, the absorption of the fundamental CO transition was saturated. Therefore, the intensity of 2ν₁ at 4250 cm⁻¹, obtained by numeric integration, was used instead. The intensities of BF₃ and complex bands were determined from the spectral region between 730 and 600 cm⁻¹. In this region, a complex pattern due to BF₃, and Fe(CO)₅ and CO₂ present as impurities,¹¹ and the complex species is observed. The complex bands were isolated by subtracting out the rescaled contribution due to BF₃, Fe(CO)₅, and CO₂, followed by a least-squares profile analysis, using Gauss-Lorentz sum bands, of the complex doublet. From the concentration variations of the relative intensities, the resulting components are easily assigned to one or another of the complex species that appear to be formed. As measure for BF₃, the integrated intensity of the 708/681 cm⁻¹ isotopic doublet was used, and the intensities of the 657 and 644 cm⁻¹ complex bands were obtained from the least-squares analysis. The latter were then plotted against the intensity products (I(BF₃))² × I(CO), I(BF₃) × I(CO), I(BF₃) × (I(CO))², and I(BF₃) × (I(CO))³. The χ² values from the linear regression of these plots are given in Table 3. The results clearly indicate that the band at 657 cm⁻¹, correlated with the band at 1489 cm⁻¹ in Figure 1, is due to the 1:1 complex, while the band at 644 cm⁻¹, correlated with the 1486-cm⁻¹ band, must be due to BF₃·(CO)₂. It is assumed that the 1:1 complex has the same structure as the complex observed in the gas phase,⁵ and that the 1:2 complex has the anticipated trigonal bipyramidal structure.

At the lowest temperatures, for solutions containing the highest concentrations of CO, problems were encountered when

Table 3. χ^2 Values for the Complex Bands at 657 and 644 cm^{-1}

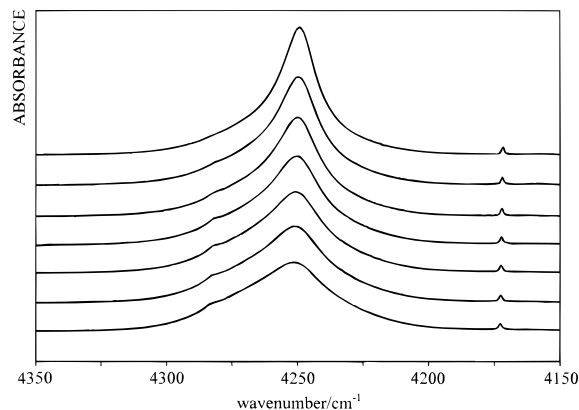
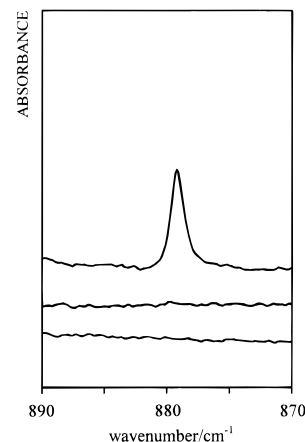
BF ₃ :CO	band at	
	657 cm^{-1}	644 cm^{-1}
2:1	483	1111
1:1	27	1478
1:2	743	306
1:3	2516	506

**Figure 2.** Superposition of the spectrum of a mixed solution with that of a solution containing only BF₃, in the region of ν_2 of monomer ¹⁰BF₃, as a function of temperature. For both solutions the concentration of BF₃ was 5×10^{-4} M, while for the mixed solution the concentration of CO was 3×10^{-1} M. The spectrum of the mixed solution appears noisier than the rescaled spectrum of the BF₃ solution, because a large fraction of the monomer has been transformed into CO complexes. From top to bottom the temperatures are 84.6, 86.6, 88.9, and 91.3 K.

the monomer ¹⁰BF₃ band at 707 cm^{-1} was simulated by rescaling the spectrum of a solution containing only BF₃: this is illustrated in Figure 2. It is clear that for the mixed solution a weak, broad band is present on the low-frequency side of the 707- cm^{-1} band. Although its intensity is difficult to quantify, from a concentration study no clear evidence was found that it originates either in BF₃·CO or in BF₃·(CO)₂. Therefore, it cannot be excluded that this band is due to a third complex species. Its intensity then suggests this species is very weakly bound. Moreover, the formation of a weak complex cannot greatly disturb the BF₃ modes: in agreement with this, the weak shoulder is situated much closer to the monomer band than those of the 1:1 and 1:2 complexes. Carbon monoxide has been observed previously to form weak complexes via its oxygen atom,^{12,13} and, therefore, we tentatively assign the weak shoulder to the 1:1 complex BF₃·OC, in which the bonding occurs between the boron and oxygen atoms.

Also for the complexes the band frequencies are temperature dependant. For the ν_2 and ν_3 bands for which the maxima can be accurately determined, the gradients of the linear regression lines are given in Table 2. It can be seen that there is a steady increase of the gradient from BF₃ to BF₃·(CO)₂.

The complexes are observed only when a substantial excess of CO is used. Under these circumstances, the fundamental monomer CO stretch is saturated over a wide frequency interval, prohibiting the stretches in the complexes to be observed. In the region of the first overtone, due to the increased frequency separation, and due to the smaller absorptivity of the monomer transition, the first overtone of the 1:1 complex was observed. In Figure 3 this region is given at several temperatures. The monomer gives rise to the band at 4250 cm^{-1} , while the weak

**Figure 3.** The region of the first overtone of the CO stretching of a solution in liquefied argon containing BF₃ (7×10^{-3} M) and CO (1×10^{-1} M), at different temperatures. From top to bottom the temperatures are 89.8, 94.9, 98.7, 103.5, 107.3, 110.0, and 114.8 K.**Figure 4.** The region of the BF₃ symmetric stretch, at 84.7 K: (top) solution in liquefied argon of a mixture of BF₃ (5×10^{-4} M) and CO (1×10^{-1} M); (middle) solution containing only BF₃ (5×10^{-4} M); (bottom) solution containing only CO (1×10^{-1} M).

transition at 4282 cm^{-1} is assigned to BF₃·CO. Because the bonding in the complex is very weak, we can neglect the change in anharmonicity of the C≡O stretch upon complexation. Then, the frequency difference of 32 cm^{-1} between the first overtones must be twice the difference between the fundamentals. The latter, therefore, is derived to be 16 cm^{-1} . Using the published liquid argon monomer frequency,¹¹ this puts the CO stretch in BF₃·CO at 2154 cm^{-1} .

For BF₃, of symmetry D_{3h} , the a_1' symmetric stretch is symmetry forbidden in the infrared. Using Raman, its frequency in the liquid phase was determined¹⁴ at 880 cm^{-1} for both ¹⁰BF₃ and ¹¹BF₃. In the C_{3v} complex BF₃·CO, the symmetric BF₃ stretch has a_1 symmetry and the fundamental is allowed in the infrared. If it is assumed that in solution the nonplanarity of the BF₃ moiety is the same as in the gas phase, it must be anticipated from the small vapor phase C–B–F angle in the complex⁵ that the intensity of this fundamental will be very low. The 900–850- cm^{-1} region of the spectrum of a concentrated BF₃/CO solution is compared with that of a solution containing only BF₃ and that of a solution containing only CO in Figure 4. In the spectrum of the mixed solution a new, weak band is present at 879 cm^{-1} , which is absent in the spectra of the other solutions. The weakness of this band is reflected from the ratio of its intensity to that of the 1489- cm^{-1} band, which was measured to be 1:720. The intensity of this band is temperature

(12) Lundell, J.; Räsänen, M.; Latajczka, Z. *Chem. Phys. Lett.* **1994**, 222, 33–39.(13) Lundell, J.; Räsänen, M. *J. Phys. Chem.* **1993**, 97, 9657–9663.(14) Steinhardt, R. G., Jr.; Fetsch, G. E. S.; Jordan, M. W. *J. Chem. Phys.* **1965**, 43, 4528–4530.

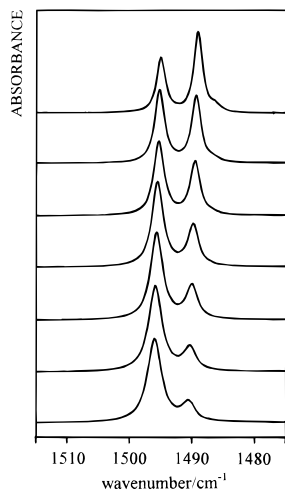


Figure 5. The region of the antisymmetric BF_3 stretch of a solution in liquefied argon containing BF_3 (5×10^{-4} M) and CO (5×10^{-2} M) as a function of temperature. From top to bottom the temperatures are 88.0, 92.1, 94.4, 98.7, 101.4, 105.6, and 108.2 K.

and concentration sensitive, as is expected for a band originating in a complex species. Therefore, we propose to assign this band to the symmetric BF_3 stretching fundamental of $\text{BF}_3 \cdot \text{CO}$. In view of the weakness of the interaction between BF_3 and CO , its position is not surprising.

C. Complexation Enthalpies. The enthalpies of complexation of the 1:1 and 1:2 complexes were determined from a temperature study. Starting from the Van't Hoff isochore, the usual analysis shows that for a complex $\text{BF}_3 \cdot (\text{CO})_n$ the following relation holds between intensities I of bands due to the different species:

$$\ln \frac{I(\text{BF}_3 \cdot (\text{CO})_n)}{I(\text{BF}_3)I(\text{CO})^n} = -\frac{\Delta H_0}{RT} + \text{constant}$$

The Van't Hoff plot obtained from a temperature study is a straight line of slope $-\Delta H_0/R$ only if ΔH_0 is sufficiently constant over the temperature interval, and if the absorptivities of the bands are sufficiently constant. In view of the frequency shifts of the bands of BF_3 with temperature, the latter condition is not evidently satisfied. The concentration of a liquid argon solution is not easily established accurately,¹⁰ and this prevents an evaluation of the absolute intensities. From Table 2 it can be seen that the temperature gradients of ν_2 and ν_3 of BF_3 are rather different, and this might lead to different temperature dependancies of the relative intensities. This was investigated by measuring the integrated intensities of the ν_2 and ν_3 isotopic doublets in liquid argon at nine different temperatures between 96 and 108 K. The linear regression of the ratios of the ν_3 and ν_2 doublets against temperature gives a direction cosine of $0.003(9) \text{ K}^{-1}$. Thus, the relative intensities of ν_2 and ν_3 do not change with temperature. Although this result cannot straightforwardly be generalized to the other intensities used in the analysis, it was seen as an indication that the temperature effects on the intensities are sufficiently small to make the present approach to measuring ΔH_0 meaningful.

For the Van't Hoff plots, in all cases for CO the first overtone was used. For the 1:1 complex the data for BF_3 and $\text{BF}_3 \cdot \text{CO}$ were taken from the region of ν_3 of $^{10}\text{BF}_3$. This region of the spectra, recorded at different temperatures, is shown in Figure 5. The intensities were measured using the least-squares band profile analysis. The 1496 cm^{-1} monomer band was used to obtain $I(\text{BF}_3)$. The strong overlap between the bands at 1489

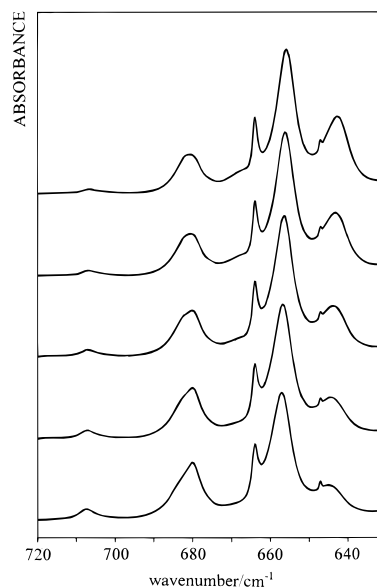


Figure 6. The region of the BF_3 out-of-plane bending of a solution in liquefied argon containing BF_3 (5×10^{-4} M) and CO (3×10^{-1} M) as a function of temperature. From top to bottom the temperatures are 84.7, 86.9, 89.1, 91.3, and 93.8 K.

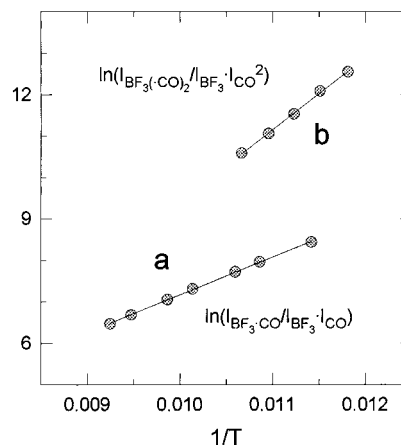


Figure 7. Van't Hoff plots for (a) the 1:2 and (b) the 1:1 complex between BF_3 and CO .

and 1486 cm^{-1} may affect the accuracy of the band profile analysis. This problem was avoided by using less concentrated solutions in which, as can be seen in Figure 5, the 1486-cm^{-1} band is very weak. Then, even when the intensity of the latter is not accurately determined by the band profile analysis, this hardly will affect the result for the 1:1 complex band at 1489 cm^{-1} .

Intensities for the 1:2 complex were taken from the $730\text{--}600\text{-cm}^{-1}$ region of solutions containing higher concentrations of the monomers. Some of the spectra, recorded at different temperatures, are shown in Figure 6. The intensities of the BF_3 band at 707 cm^{-1} and of the $\text{BF}_3 \cdot (\text{CO})_2$ band at 644 cm^{-1} were determined by the procedure used in the concentration study. Problems with the low-frequency shoulder on the 707-cm^{-1} band, discussed above, were avoided by using less concentrated solutions.

The Van't Hoff plots are shown in Figure 7. For both complexes a highly linear relationship is obtained. From the linear regression, the enthalpy of complexation ΔH_0 was determined to be $-7.6 \pm 0.3 \text{ kJ mol}^{-1}$ for the 1:1 complex and $-14.5 \pm 1.0 \text{ kJ mol}^{-1}$ for the 1:2 complex.

Table 4. Frequencies, Solvent Shifts, and Complexation Shifts, in cm^{-1} , for ν_2 and ν_3 in BF_3 and Its CO Complexes in Liquid Argon at 85 K

	BF_3		$\text{BF}_3\cdot\text{CO}$		$\text{BF}_3\cdot(\text{CO})_2$	$\Delta\nu_c(1:1)$	$\Delta\nu_c(1:2)$
	freq	$\Delta\nu_s(\text{BF}_3)$	freq	$\Delta\nu_s(\text{BF}_3\cdot\text{CO})$			
$\nu_3(^{10}\text{B})$	1495.00	-10.78	1488.97	-8.75	1486.11	-6.03	-8.89
$\nu_3(^{11}\text{B})$	1443.75	-10.22	1437.95	-7.10	1435.05	-5.80	-8.70
$\nu_2(^{10}\text{B})$	707.02	-12.27					
$\nu_2(^{11}\text{B})$	679.50	-11.71	656.27	-7.76	642.60	-23.23	-36.90

^a $\Delta\nu_s = \nu_s - \nu_g$ (s: solution; g: gas). ^b $\Delta\nu_c(1:1) = \nu_s(\text{BF}_3\cdot\text{CO}) - \nu_s(\text{BF}_3)$. ^c $\Delta\nu_c(1:2) = \nu_s(\text{BF}_3\cdot(\text{CO})_2) - \nu_s(\text{BF}_3)$.

Discussion

In the discussion below, for simplicity, for the CO complexes we will use the same numbering for the BF_3 modes as in the monomer, i.e. the BF_3 antisymmetric stretch will always be indicated as ν_3 and the BF_3 out-of-plane deformation as ν_2 .

In Table 4 the observed frequencies for ν_2 and ν_3 in BF_3 , $\text{BF}_3\cdot\text{CO}$, and $\text{BF}_3\cdot(\text{CO})_2$ in argon at 85 K are collected, together with the solvent shifts $\Delta\nu_s = \nu_{\text{solution}} - \nu_{\text{gas}}$, for BF_3 and $\text{BF}_3\cdot\text{CO}$, and the complexation shifts $\Delta\nu_c = \nu_{\text{complex}} - \nu_{\text{monomer}}$, for the 1:1 and 1:2 complexes. These data, for instance, show that in solution the shift of ν_2 of $^{11}\text{BF}_3$ upon complexation to $\text{BF}_3\cdot\text{CO}$ equals -23.23 cm^{-1} , while for ν_3 it is -5.8 cm^{-1} . In the vapor phase⁷ these shifts are -27.18 and -7.92 cm^{-1} , respectively. The substantial solvent influences apparent from these data can be qualitatively understood from a relatively simple model. This, in the first instance, requires that CO and the solvent shifts for the monomer BF_3 frequencies are rationalized.

In a reaction field¹⁵ description, using a spherical cavity for the solute molecule, the solvent shift of an infrared band is proportional to $(\partial\bar{\mu}/\partial Q)_0^2$, i.e. to the intensity of the band. Using relative intensities measured in liquefied argon, it is then predicted that the shift of ν_3 should exceed that of ν_2 by a factor of 6. It can be seen in Table 4 that, in fact, they are smaller. This failure of the reaction field description shows that local order in the solutions¹⁶ dominates the shifts. In the vapor phase Van der Waals complex $\text{BF}_3\cdot\text{Ar}$, the argon atom is located on the threefold axis of the BF_3 moiety.⁵ The existence of such a structurally well-defined complex suggests that the potential energy surface for interaction of BF_3 with Ar shows a minimum of appreciable depth around the threefold axis, and this on either side of the BF_3 molecule. This imposes the local order around BF_3 in an argon solution: as a consequence of the potential well, at any instant of time there is a high probability of finding an argon atom at, or near, the threefold axis, on either side of BF_3 . Although this must be interpreted dynamically, for the present purpose it is instructive to extrapolate it to assuming that in solution BF_3 occurs as a 1:2 Van der Waals complex $\text{BF}_3\cdot(\text{Ar})_2$. For all other solvent atoms it will be assumed that they are evenly distributed around the $\text{BF}_3\cdot(\text{Ar})_2$ entity, creating a spherical solvation shell.

For a quantitative discussion of the solvent shifts induced by the axial argon atoms, comparison with gas-phase data on ν_2 and ν_3 in $\text{BF}_3\cdot(\text{Ar})_2$ is necessary. Unfortunately, no studies of this complex have been published. However, high-resolution infrared spectra of $\text{BF}_3\cdot\text{Ar}$ have been investigated^{17,18} in the

regions of ν_2 and ν_3 , and we will interpret our solution frequencies in terms of these data.

In the gas phase,¹⁷ $\nu_3(^{11}\text{B})$ shifts by -1.7609 cm^{-1} from BF_3 to $\text{BF}_3\cdot\text{Ar}$, while the shifts for $\nu_2(^{10}\text{B})$ and $\nu_2(^{11}\text{B})$ are¹⁸ -6.0022 and -5.7099 cm^{-1} , respectively. In the inductive model of Lee et al.,¹⁸ this considerable mode specificity is explained by the orientation of the vibrational dipole gradient relative to the static dipole moment induced by the partial charges on B and F atoms in the argon atom. For ν_3 , the gradient is oriented perpendicular to the static induced dipole moment, while for ν_2 it is parallel with it, allowing the $\nu = 1$ state of ν_2 to be stabilized much more than the corresponding state of ν_3 , leading to the observed difference in the frequency shifts.

It is not easy to infer from the gas-phase complexation shifts of $\text{BF}_3\cdot\text{Ar}$ the shifts of ν_2 and ν_3 in $\text{BF}_3\cdot(\text{Ar})_2$. However, they must fall between those for $\text{BF}_3\cdot\text{Ar}$ and twice these values. This appears to be confirmed by the complexation shifts for $\text{BF}_3\cdot(\text{CO})_2$ given in Table 4, even if, as will be discussed below, these shifts must be put in the proper perspective. The shifts for the latter complex are roughly 1.5 times those for the corresponding 1:1 complex. If we use this factor for the argon complexes, for $\text{BF}_3\cdot(\text{Ar})_2$ the shift predicted for $\nu_2(^{11}\text{B})$ is -9.0 cm^{-1} , and -2.6 cm^{-1} for $\nu_3(^{11}\text{B})$. Within the model described above, these values must be regarded as the upper limits of the shifts induced in solution by the axial argon atoms.

As to the influence of the solvation shell, argon atoms in the shell that are near or in the BF_3 plane must induce appreciable shifts in ν_3 , but much smaller shifts in ν_2 . Finally, solvation shell atoms near the C_3 axis, which necessarily are at a very large distance from the boron atom, will have minor influences on both ν_2 and ν_3 . It must, therefore, be expected that the ratio of the gas-to-solution shifts of ν_3 to ν_2 will be significantly bigger than that of the gas-phase monomer-to-complex shifts.

The solvent shifts for ν_2 given in Table 4 are somewhat larger than the predicted upper limits of the shifts induced by the axial argon atoms: this shows that the latter dominate the shifts but that the solvation shell has a minor but non-negligible influence on the measured frequencies. In contrast, the observed solvent shifts for ν_3 , on average -10.5 cm^{-1} , are much larger than the upper limit of the shifts induced by the axial argon atoms: in agreement with the above expectations, it is clear that for this mode the largest contribution to the shift is due to the solvation shell.

It was observed above that in solution the BF_3 bands shift linearly with temperature. This must be attributed to two contributions. First, at higher temperatures the mobility of the axial argon atoms increases, and this will increase the average distance between the argon and the boron atoms. Secondly, the rather pronounced thermal expansion of argon solutions causes an increase in the solvation shell diameter, increasing the average distance between BF_3 and the shell atoms. Both effects must lead to a decrease in solvent shift. The experimental observations are in agreement with this.

(15) Bulanin, M. O.; Orlova, N. D.; Zelikina, G. Ya. In *Molecular Cryospectroscopy*; Clark, R. J. H., Hester, R. E., Eds.; J. Wiley and Sons: Chichester, 1995; pp 35–87.

(16) Zimmerman, H. W. In *Organic Liquids, Structure, Dynamics, and Chemical Properties*; Buckingham, A. D., Lippert, E., Bratos, S., Eds.; J. Wiley and Sons: Chichester, 1978; pp 1–47.

(17) Matsumoto, Y.; Ohshima, Y.; Takami, M.; Kuchitsu, K. *J. Chem. Phys.* **1989**, *90*, 7017–7021.

(18) Lee, G.-H.; Matsuo, Y.; Takami, M.; Matsumoto, Y. *J. Chem. Phys.* **1992**, *96*, 4079–4087.

(19) Yamamoto, S.; Kuchitsu, K.; Nakanaga, T.; Takeo, H.; Matsumura, C.; Takami, M. *J. Chem. Phys.* **1986**, *84*, 6027–6033.

For both ν_2 and ν_3 the vibrational dipole moment is for the larger part determined by the motion of the boron atom.¹⁸ Consequently, the vibrational dipole moment and, therefore, the solvent shifts must be boron-isotope sensitive.¹⁸ The data in Table 4 indicate that the modes in $^{10}\text{BF}_3$ show a slightly bigger solvent shift than those in $^{11}\text{BF}_3$. At 85 K, the ratio of the solvent shifts is 1.055(3) for ν_3 , while for ν_2 it is 1.048(3). The latter value is close to that found for $\text{BF}_3\cdot\text{Ar}$.¹⁸ Table 2 shows that the components of the isotopic doublets have different temperature gradients. The differences, however, are small, so that throughout the temperature interval studied, the order of the shifts remains unaltered. Obviously, these observations confirm the anticipated isotope effect.

In terms of the solvation model, the formation of a 1:1 complex $\text{BF}_3\cdot\text{CO}$ in solution is the substitution of one of the axial argon atoms by a CO molecule. If it is assumed that this substitution does not alter the solvation shell, then the complexation shifts in liquid argon must be the same as the vapor phase shifts from $\text{BF}_3\cdot\text{Ar}$ to $\text{BF}_3\cdot\text{CO}$. In the gas phase, the shift of ν_2 from $^{11}\text{BF}_3\cdot\text{Ar}$ to $^{11}\text{BF}_3\cdot\text{CO}$ is obtained by subtracting the shift from $^{11}\text{BF}_3$ to $^{11}\text{BF}_3\cdot\text{Ar}$, -5.710 cm^{-1} ,¹⁸ from the shift from $^{11}\text{BF}_3$ to $^{11}\text{BF}_3\cdot\text{CO}$, -27.180 cm^{-1} ,⁷ giving -21.470 cm^{-1} . As said above, the gas-phase $\text{BF}_3\cdot\text{Ar}$ complexation shift is an upper limit for the solvent shift induced by an axial argon atom: therefore, the complexation shift in solution must be expected to be somewhat larger than -21.47 cm^{-1} . The experimental value, -23.23 cm^{-1} , indeed is close to, but somewhat larger than, the predicted shift.

For $\nu_3(^{10}\text{B})$ in the same way for the vapor phase a $\text{BF}_3\cdot\text{Ar}$ to $\text{BF}_3\cdot\text{CO}$ shift equal to -6.159 cm^{-1} is calculated from the published data.^{7,17} In very good agreement with this value, in liquid argon a frequency difference of -6.03 cm^{-1} is found.

The data in Table 4 show that for ν_3 , for which data for both isotopic BF_3 species are available, the shifts for the 1:1 as well as for the 1:2 complex show the expected boron isotope effect.

In contrast to the modes localized in BF_3 , it was shown above that the $\text{C}\equiv\text{O}$ stretching in the complex is at higher frequency than in the monomer. The bonding between boron and carbon atoms occurs via the $\text{sp}\sigma^*$ HOMO orbital of CO. The decreasing population of this antibonding orbital in the complex strengthens the $\text{C}\equiv\text{O}$ bond, giving rise to the observed blue shift of 16 cm^{-1} .

In the high-resolution infrared study of $\text{BF}_3\cdot\text{CO}$, anomalous fine structure, presumably chaotic in nature, has been observed⁷ for $\nu_2(^{11}\text{B})$ and $\nu_3(^{11}\text{B})$, which is absent in $\nu_2(^{10}\text{B})$ and $\nu_3(^{10}\text{B})$. Although in solution the rotational fine structure of the complexes has collapsed, a strong perturbation of the rotational behavior might reveal itself through the bandwidth of the observed vibrational bands. No such effects, however, are observed in our spectra. This is not really surprising, as in $\nu_2(^{11}\text{B})$ and $\nu_3(^{11}\text{B})$ the overall symmetric-top characteristics are preserved, showing that the perturbation causing the anomalous splitting is very weak and cannot be detected in the low-resolution spectra studied here.

Finally, it was argued in the introduction that the bonding strength of the second CO in $\text{BF}_3\cdot(\text{CO})_2$ should be similar to that of the first one. This appears to be borne out by the enthalpy differences, even if we allow for the fact that these quantities are not exclusively determined by the energetics of the bonds: the complexation enthalpy for the 1:2 complex indeed is almost twice the value for the 1:1 complex.

Acknowledgment. This research was performed with financial support of the Flemish Institute for the Promotion of Scientific-Technological Research in the Industry (IWT). The NFWO is thanked for financial support toward the spectroscopic equipment used in this study.

JA950443G